Heliyon 11 (2025) e42457

Contents lists available at ScienceDirect

Heliyon

journal homepage: www.cell.com/heliyon

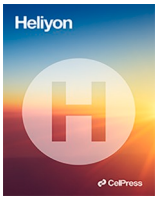

Research article

Pharmacological inhibition of carbonic anhydrases with a positively charged pyridinium sulfonamide phenocopies the neuroprotective effects of *Car9* genetic ablation in a murine setting of oxygen/glucose deprivation followed by re-oxygenation and is associated with improved neuronal function in ischemic rats

Sara Amiranda [a,b,1], Mariangela Succoio [a,b,1], Serenella Anzilotti [c,1], Ornella Cuomo [d], Tiziana Petrozziello [d], Valentina Tedeschi [d], Arianna Finizio [a,b], Giorgia Mele [a,b], Seppo Parkkila [e,f], Lucio Annunziato [g], Giuseppina De Simone [h], Giuseppe Pignataro [d], Agnese Secondo [d,**], Nicola Zambrano [a,b,*]

[a] *Dipartimento di Medicina molecolare e Biotecnologie mediche, Università degli Studi di Napoli Federico II, Napoli, Italy*
[b] *CEINGE Biotecnologie Avanzate Franco Salvatore S.C.aR.L., Napoli, Italy*
[c] *Department of Human Sciences and Quality of Life Promotion, Università San Raffaele, Rome, Italy*
[d] *Division of Pharmacology, Dipartimento di Neuroscienze e Scienze Riproduttive ed Odontostomatologiche, Università degli Studi di Napoli Federico II, Napoli, Italy*
[e] *Faculty of Medicine and Health Technology, Tampere University, Tampere, Finland*
[f] *Fimlab Ltd, Tampere University Hospital, Tampere, Finland*
[g] *SYNLAB SDN, Via Gianturco, Napoli, Italy*
[h] *Istituto di Biostrutture e Bioimmagini, CNR, Via Pietro Castellino 111, 80131, Napoli, Italy*

ARTICLE INFO

Keywords:
Hypoxia
Brain ischemia
Carbonic anhydrase IX
Carbonic anhydrase inhibitors

ABSTRACT

Carbonic anhydrases constitute a family of metalloenzymes vital for maintaining acid-base balance and regulating pH in physio-pathological processes. These findings suggest carbonic anhydrases as potential therapeutic targets for treating pH-associated disorders, including cerebral ischemia, to mitigate hypoxia- and reoxygenation-induced neuronal damage. A focus on carbonic anhydrase IX showed that ischemic stress altered subcellular distributions of this enzyme in rodent neuronal populations. Given the enzyme's canonical membrane localization, we implemented pharmacological inhibition using a membrane-impermeant sulfonamide inhibitor in neuronal models of brain ischemia. The treatments exerted neuroprotective effects on neurons from *Car9* knockout mice. Moreover, administration of the sulfonamide inhibitor to rats subjected to transient middle cerebral artery occlusion decreased infarct volumes and improved neurological deficits. Our results support the involvement of carbonic anhydrase IX in postischemic

Abbreviations: CA, carbonic anhydrase; CAI, carbonic anhydrase inhibitor; C18, sulfonamidic compound 18; OGD, oxygen-glucose deprivation; KO, knock-out; Rx, re-oxygenation; tMCAO, transient middle cerebral artery occlusion.

* Corresponding author. Dipartimento di Medicina molecolare e Biotecnologie mediche, Università degli Studi di Napoli Federico II, Napoli, Italy.
** Corresponding author.
E-mail addresses: agnese.secondo@unina.it (A. Secondo), zambrano@unina.it (N. Zambrano).
[1] Equal contribution.

https://doi.org/10.1016/j.heliyon.2025.e42457
Received 3 June 2024; Received in revised form 30 January 2025; Accepted 3 February 2025
Available online 5 February 2025

damage and pave the way for possible pharmacological interventions with selective inhibitors in the management of brain ischemia.

Carbonic anhydrases (CAs) belong to a superfamily of ubiquitous metalloenzymes present in prokaryotes and eukaryotes, which are encoded by evolutionarily unrelated gene families [1]. All human CAs (hCAs) belong to the so-called α-class and widely differ in subcellular localization, tissue distribution, and catalytic activity [2]. CAs catalyse the reversible conversion of carbon dioxide and water in bicarbonate and protons, playing crucial roles in crucial physiological and pathological processes linked to pH and CO2 homoeostasis and sensing [1–3]. Hence, CAs are considered valuable therapeutic targets for disorders associated with pH imbalances. So far, two main strategies have been used to inhibit CAs, particularly CA IX: the development of small molecule inhibitors and the design of monoclonal antibodies [4,5]. In this light, understanding the structure and mechanism of action of these enzymes has provided important perspectives into designing selective CA inhibitors (CAIs) with potential diagnostic and therapeutic applications [6].

A crucial problem of CA inhibition is the presence of several isoforms that differ in localization but share high similarity in their activities [4–7]. The first class of CAIs, which includes acetazolamide and its derivates, consist of highly efficient compounds acting in the nanomolar range. However, these compounds lack selectivity among different isoforms, which could lead to a range of undesired side effects [2]. Considerable effort has been implemented, to reduce these potential side effects and to enhance selectivity for CA IX inhibition [7]. This includes the design of membrane-impermeable compounds, specifically inhibiting the membrane-associated isoforms, such as CA IV, CA IX, CA XII, and CA XIV, without interacting with intracellular ones. One such compound is 1-N-(4-sulfamoylphenyl-ethyl)-2,4,6-trimethylpyridinium perchlorate, hereafter indicated as compound 18 (C18) [8]. As described in detail by Supuran and coworkers [1,9,10], C18 benefits from its positive charge and pyridinium moieties, allowing it to selectively target membrane-associated CAs due to its inability to cross the plasma membrane.

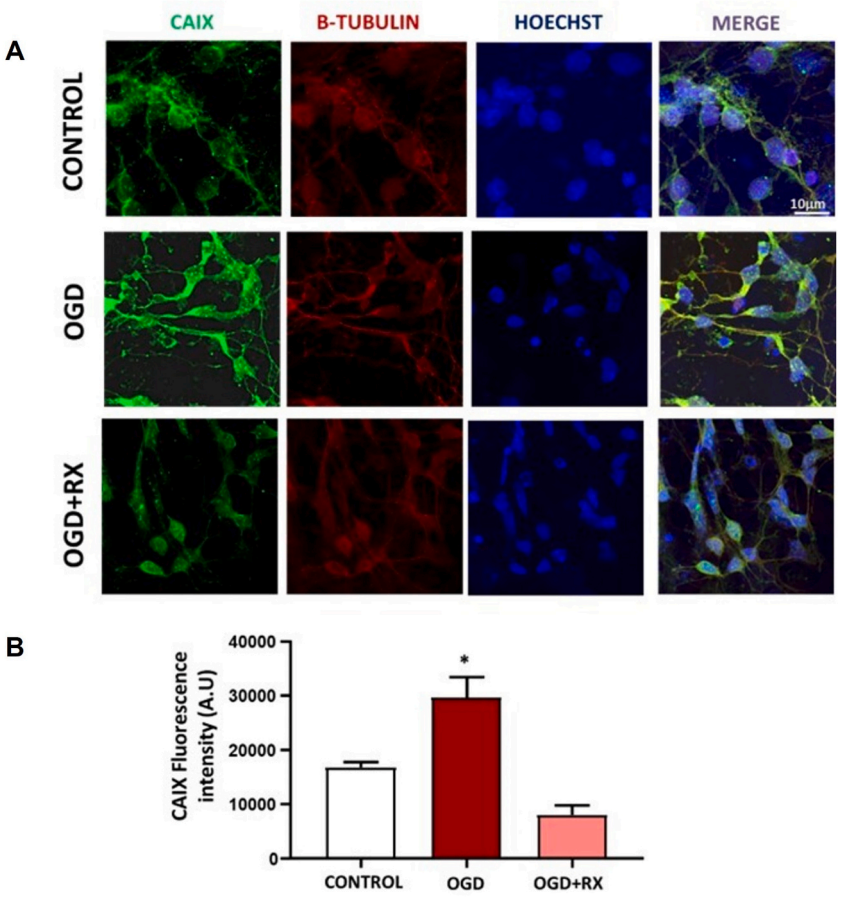

Fig. 1. CA IX (Car9) expression in the experimental setting of primary rat cortical neurons exposed to Oxygen Glucose Deprivation followed by Re-oxygenation. (A) Immunofluorescence analysis showing CAIX (green), β-tubulin (red), and Hoechst (blue) under normal conditions, OGD, and OGD/Rx. (B) Quantification of CAIX fluorescence intensity, expressed in arbitrary units (AU). Data are expressed as mean ± SEM (n = 3/4 for each group). *$p < 0.05$ Error bars ± SEM; statistical significance was assesses using a one-way ANOVA test with Tukey's multiple comparisons test, df = 9.

Beyond its well-known role in tumours [11–14], cellular hypoxia is a key feature of other significant pathological conditions, including brain ischemia [15]. Currently, the most commonly used treatment for ischemic stroke is thrombolytic therapy; but only 10 % of patients are eligible for this therapy. To date, many therapeutic agents are in clinical or preclinical studies for the evaluation of efficacy in ischemic stroke. Despite this, the development of clinically effective neuroprotective drugs is still elusive. Rapid neuronal cell death, limited spontaneous recovery and the lack of effective therapeutic strategies contribute to this challenge [16].

Under ischemic conditions, brain acidosis generates free radicals, affects glutamate release and reuptake, determines gliosis and neuronal apoptosis [17] thus resulting in cerebral infarction characterized by oedema and blood-brain barrier dysfunction [18]. In this respect, CAs inhibition may contribute to the maintenance of pH homeostasis in the brain [19]. Accordingly, evidence suggests the possible involvement of CAs in brain ischemia, a pathological condition marked by significant acidification in affected brain areas [15]. The first evidence is that mice lacking CA II are more resistant to hypoxia-induced neuronal damage [20]. Furthermore, hypoxic conditions elicit the overexpression of CA IX and CA XII, via the hypoxia-inducible factor (HIF-1α) [21–23]. Mechanistically, CA inhibition may reduce neuronal apoptosis stabilizing pH [24]. CAs also play a role in the regulation of body fluid volumes [25], and oedema is an aggravating factor in brain ischemia. As a matter of fact, previous research has shown that sulfonamide and coumarin-based CAIs enhance outcomes in cerebral ischemia models [26]. Additionally, targeted inhibition of CA I, CA II, CA IX, and

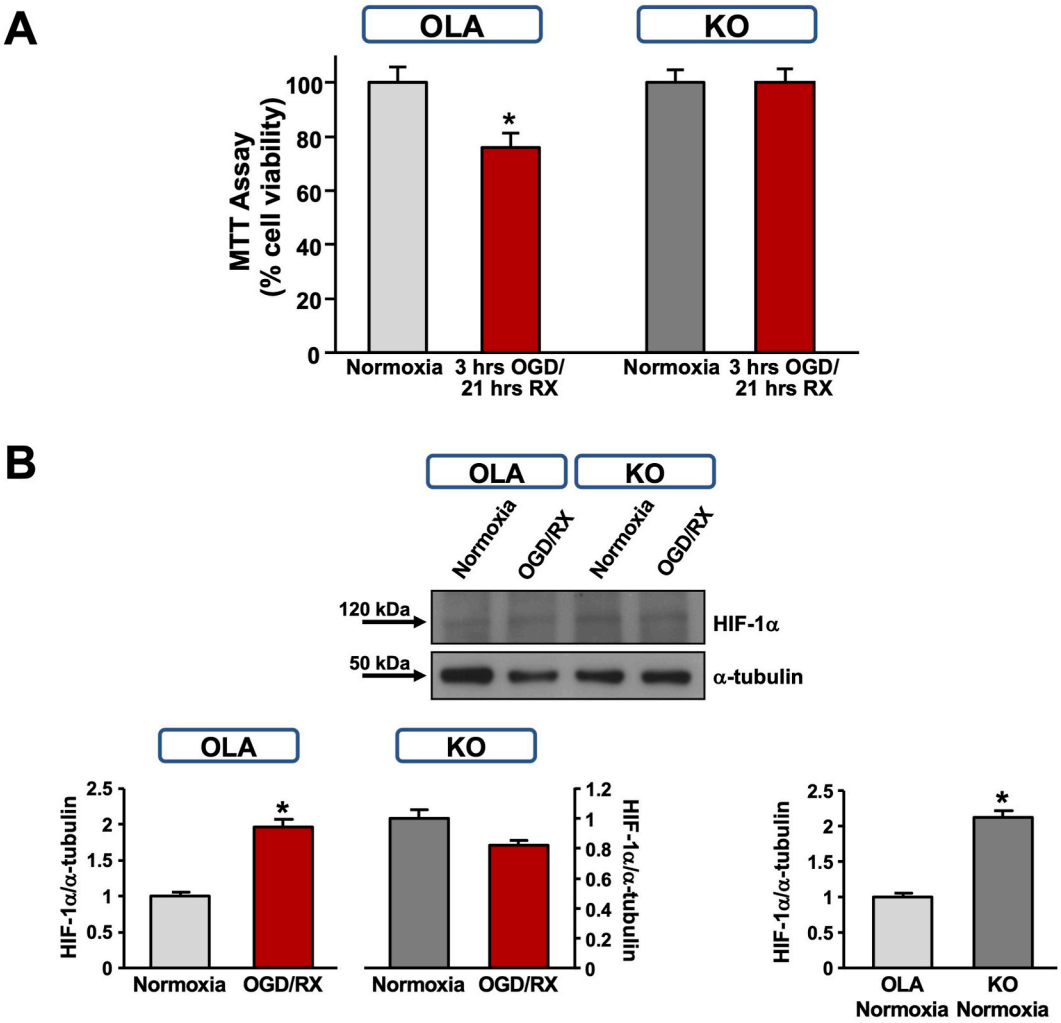

Fig. 2. Functional characterization of the genetic ablation of *Car9* in the OGD/Rx experimental setting. (A) Cell Viability analysis of primary cortical neurons from wild-type (OLA) and *Car9*-KO (KO) mice. MTT assay of mouse primary cortical neurons exposed to 3 h of OGD followed by 21 h of Rx (red bars). Experiments were repeated at least 3 times with different cultures. For each experimental group, normoxic cells (light and dark gray, respectively, for wild-type and *Car9*-KO mice) were used as control. Statistical comparisons were performed by unpaired *t*-test (*$p < 0.05$ vs normoxia; $df_{TOT} = 9$ for OLA). (B) Representative Western blotting and quantification of full-length HIF-1α in lysates of primary cortical neurons from wild-type (OLA) and *Car9*-KO (KO) mice under normoxic (light and dark gray, respectively, for wild-type and *Car9*-KO mice)or OGD/Rx conditions (3 h OGD + 21 h Rx, red bars). α-tubulin antibody was used as a loading control; experiments were repeated with different samples (*$p <$ 0.05 vs normoxia for b; *$p < 0.05$ vs OLA; dfTOT = 4). The uncropped image is provided in the supplementary materials.

CA XII has been found to significantly improve both the structural integrity and functional recovery of the ischemic brain [27,28].

Based on this rationale, we focused primarily on evaluating the role of CA IX in responses to hypoxic insults through in *vitro* and in *vivo* models of brain ischemia [29,30]. For the in *vitro* study we exploited primary cortical neurons exposed to oxygen and glucose deprivation (OGD), a well-established model for mimicking cerebral ischemia [31–35]. During OGD, the deprivation of oxygen and glucose induces a sub-lethal attack to neurons, leading to initial mitochondrial dysfunction. Subsequently, reoxygenation, which mimics the reperfusion phase that follows the restoration of cerebral blood flow, exacerbates cellular dysfunction and promotes cell death [36–38]. For the in *vivo* analysis we performed transient middle cerebral artery occlusion (tMCAO) and administered C18 intracerebroventricularly [38,39].

By integrating enzyme inhibition analysis with C18 with the genetic ablation of the murine CA IX gene orthologue, *Car9*, we provide evidence for the pivotal roles of CA IX in the responses to ischemic insults in *vitro* and in *vivo*.

1. Results

1.1. Oxygen-glucose deprivation and reoxygenation alter CA IX subcellular localization in rat primary cortical neurons

Although CA IX is particularly studied in cancer for its expression and activity in the hypoxic areas of tumours, its role in cell survival mechanisms following ischemic insults is not well understood. To address this, we examined the behaviour of endogenous CA IX protein in rat cortical neurons and subjected to ischemia-mimicking conditions. Rat primary cortical neurons were analysed by immunofluorescence using the neuronal marker βIII-tubulin, and for CA IX expression (Fig. 1A). In normoxia, CA IX protein was expressed at low levels and mainly localized on the plasma membrane. In neurons exposed to OGD, CA IX immunosignaling increased in neuronal projections, and spotted enrichments appeared at the level of nuclei. With reoxygenation (Rx), CA IX immunosignaling overall decreased, with a localization becoming prevalently nuclear (OGD/Rx) (Fig. 1B).

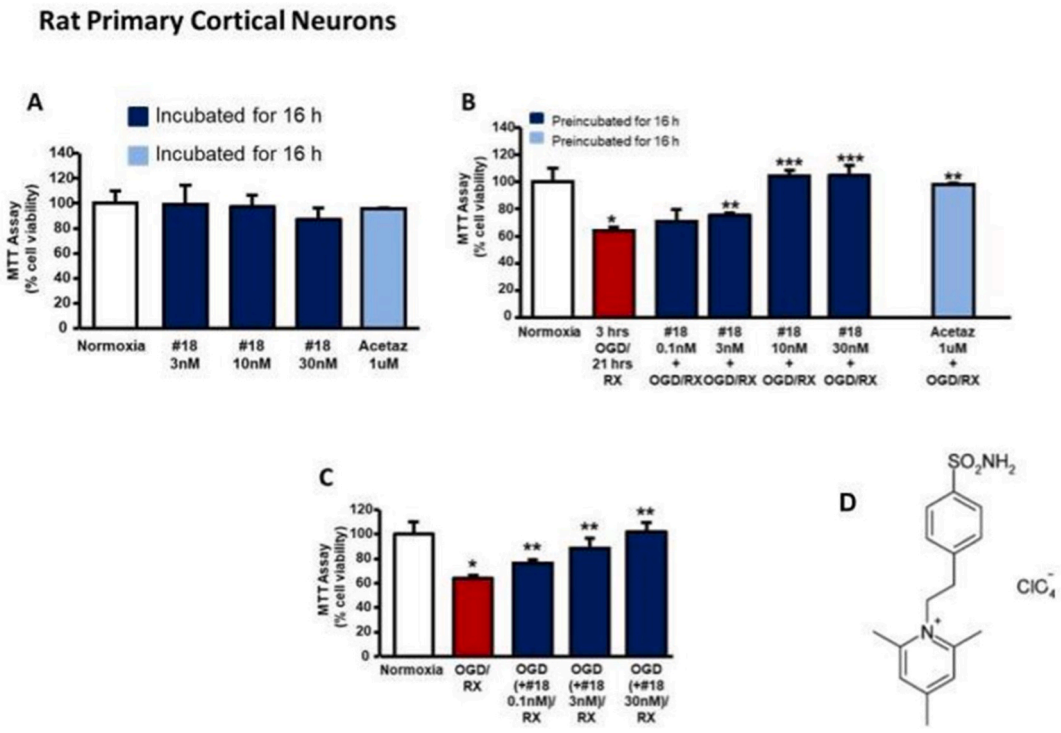

Fig. 3. Cell viability analysis of rat cortical neurons exposed to OGD and treated with C18. A) Toxicology analysis of cells treated with C18 at 3 nM, 10 nM, and 30 nM (blue) and acetazolamide at 1 μM (light blue). B) MTT analysis of cells preincubated for 16h with 0.1 nM, 3 nM, 10 nM, and 30 nM C18 (blue) and 1 μM acetazolamide (light blue) or without compounds (red) and then exposed for 3 h to OGD followed by 21h of Rx. Statistical comparisons between groups were performed by one-way ANOVA followed by Newman-Keuls' test. (*$p < 0.05$ vs normoxia; **$p < 0.05$ vs OGD/Rx; ***$p < 0.05$ vs all; $df_{TOT} = 25$). C) MTT analysis of cells exposed to OGD plus C18 at 0.1 nM, 3 nM, and 30 nM concentrations (blue) or no compound (red) followed by Rx. Normoxic cells (white) were used as control in all the assays. Statistical comparisons between groups were performed by one-way ANOVA followed by Newman-Keuls' test. (*$p < 0.05$ vs normoxia; **$p < 0.05$ vs OGD/Rx; $df_{TOT} = 17$). D) Chemical structure of C18 [10].

1.2. The sulfonamide C18 phenocopies the neuroprotection observed in primary cortical neurons from mice lacking CA IX in a setting of oxygen/glucose deprivation followed by re-oxygenation

To investigate CA IX function during brain ischemia, we used genetically modified mice with the *Car9* gene inactivated by homologous recombination [40]. In brief, the first exon of *Car9*, which encodes the signal peptide and the N-terminal region of the PG domain, was interrupted by inserting a 1.8 kilobase PGK-NEO cassette, thereby blocking the translation of the full-length protein. Notably, mouse primary cortical neurons from *Car9*-KO mice showed greater resistance to hypoxia after 3 h of OGD followed by reoxygenation, compared to wild-type neurons, which experienced significant mitochondrial dysfunction under hypoxic conditions, albeit at a lower severity (Fig. 2A). This protocol helped reveal the neuronal role of CA IX under hypoxic conditions. Further analysis of the mechanism behind the hypoxic tolerance in *Car9*-KO mice revealed that, under normoxic conditions, primary cortical neurons from these mice expressed higher level of HIF1α than their wild-type counterpart. Of note, HIF1α expression did not change in *Car9*-KO neurons under hypoxic conditions (Fig. 2B). On the other hand, wild-type neurons showed a significant increase in HIF1α expression when exposed to OGD followed by reoxygenation (Fig. 2B) as occurs in mice subjected to brain ischemia model [41]. The results from cell survival analysis suggest that CA IX plays a detrimental role in ischemic conditions. While replicating this setting in mouse embryo fibroblasts, with the aim to establish a stable and surrogate model for experimentation without the need for continuous samplings, no differences were observed between wild-type and *Car9*-KO cultures (data not shown).

The positively charged pyridinium sulfonamide C18 (Fig. 3D) inhibits carbonic anhydrases and, due to its limited cell permeability, targets extracellularly exposed enzymes, such as CA IX and CA XII with high specificity (Ki = 14 nM and 7 nM respectively) [1]. Accordingly, we characterized its potential in the hypoxia/reoxygenation setting (Fig. 3). First of all, the toxicity of the compound was assessed in rat primary cortical neurons exposed to different concentrations of C18. The MTT assay showed no toxicity at 3 nM, 10 nM, and 30 nM, with cellular viability similar to the untreated controls. Acetazolamide, a membrane-permeant, non-selective CAs inhibitor was used for comparison (Fig. 3A). To test the effect of the C18 in a hypoxic setting, primary cortical neurons were pre-treated with different concentrations of C18 for 16 h, followed by 3 h of OGD and 21 h of reoxygenation. C18 provided progressive protection under hypoxic conditions compared to untreated neurons exposed to OGD and reoxygenation (Fig. 3B). Notably, C18 showed the same protective effect when administered during the OGD phase (Fig. 3C).

To further investigate C18 potential off-target effects, *Car9*-KO neurons were pre-treated with more drastic conditions of C18 (100 nM for 16 h) before OGD and reoxygenation. In wild-type primary neurons C18 treatment led to significant recovery of neuronal viability (Fig. 4A), whereas no such difference was observed in *Car9*-KO neurons (Fig. 4B). This indicates that the observed neuroprotection is mainly due to CA IX inhibition, rather than to off-target players. Overall, these results suggest that inhibiting extracellular carbonic anhydrases, particularly CA IX, plays a crucial role in mitigating OGD/Rx stress and could offer neuroprotection in ischemic conditions.

1.3. CA IX expression in the ischemic brain

Although CA IX expression in the brain was previously reported [40], we established its neuronal localization in different brain regions by means of co-immunolocalization with the neuronal marker Neuregulin (NeuN). Striatum and motor cortex showed high expression of CA IX. Additionally, Purkinje cells of the cerebellum showed moderate CA IX expression, and the protein was also found in the hippocampus and brainstem (Fig. 5).

To investigate whether CA IX expression was altered during brain ischemia, we analysed CA IX immunosignaling in rats subjected to tMCAO focusing on the brain regions mostly affected by ischemic conditions (Fig. 6). At 24 h post-tMCAO, CA IX immunosignaling

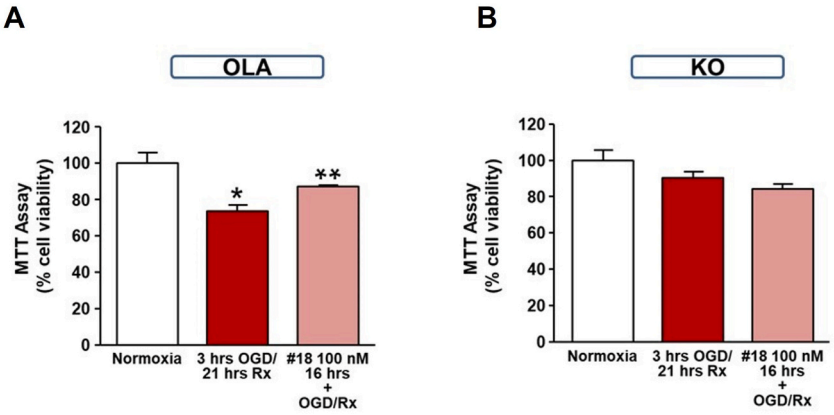

Fig. 4. Cell Viability analysis of primary cortical neurons from wild-type (OLA, panel A) and *Car9*-KO (KO, panel B) mice exposed to OGD and treated with C18. MTT analysis of mouse primary cortical neurons exposed to 3 h of OGD and 21 h of Rx (red bars) or preincubated for 16 h with 100 nM C18 and then exposed for 3 h to OGD and 21 h of Rx (light red). Normoxic cells (white) were used as control for OGD/Rx. Statistical comparisons were performed by unpaired *t*-test (*$p < 0.05$ vs normoxia; **$p < 0.05$ vs all; $df_{TOT} = 9$).

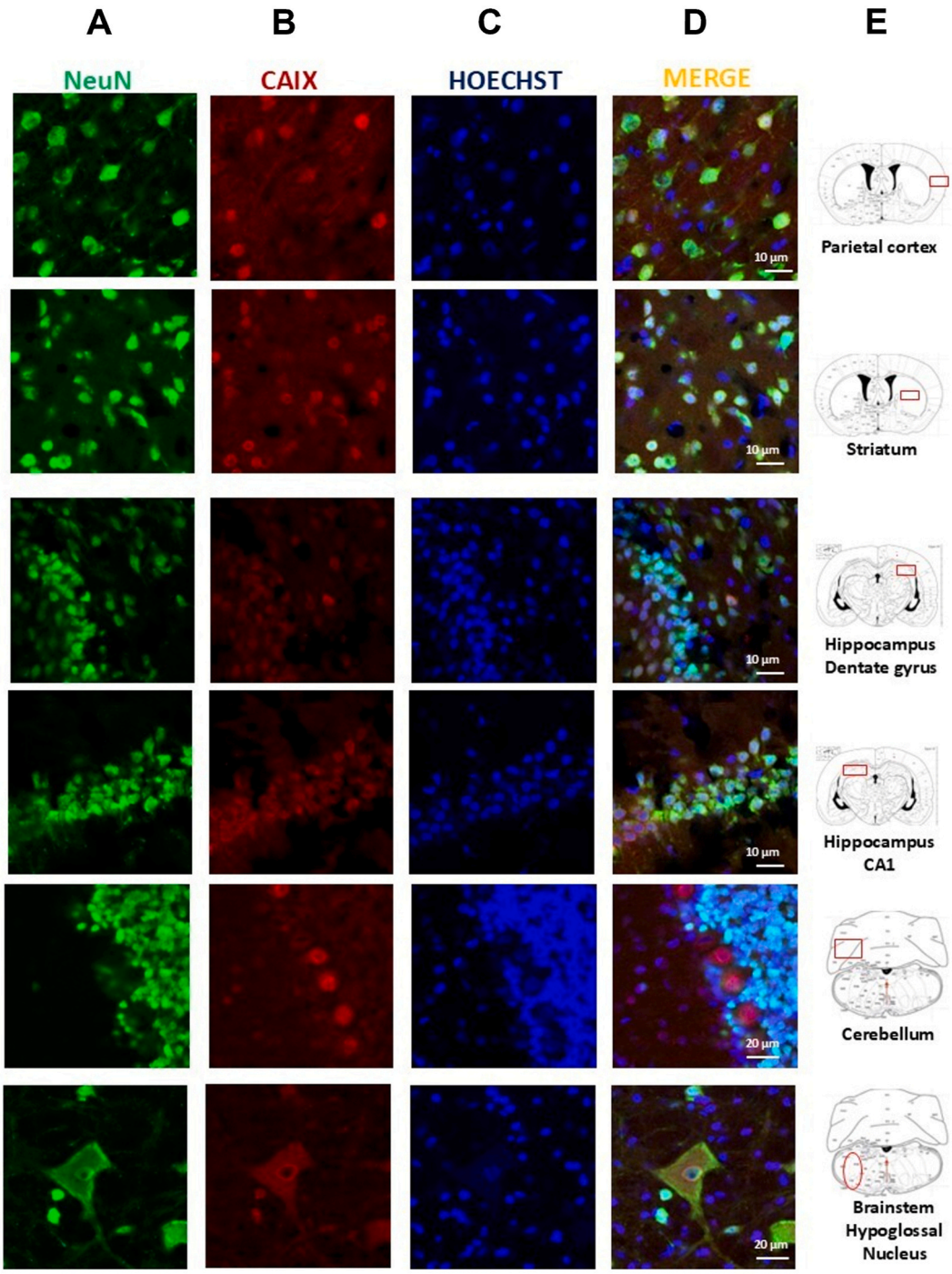

Fig. 5. Immunofluorescence analysis of CAIX expression in brain regions. NeuN (Neuronal marker, green, column A), CA IX (red, column B), Hoechst (blue, column C), and merged images (column D) in non-ischemic rats. Cartoons and red boxes on the right side (column E) indicate the brain regions examined.

decreased in the ipsilateral cortex (Fig. 6A) and striatum (Fig. 6B) compared to the contralateral side.

Interestingly, at 6 h post-tMCAO, CAIX immunosignaling in the same brain regions appeared slightly increased and revealed co-expression with Exportin 1 (CRM1) in cells positive for CRM1 (Fig. 7A and B).

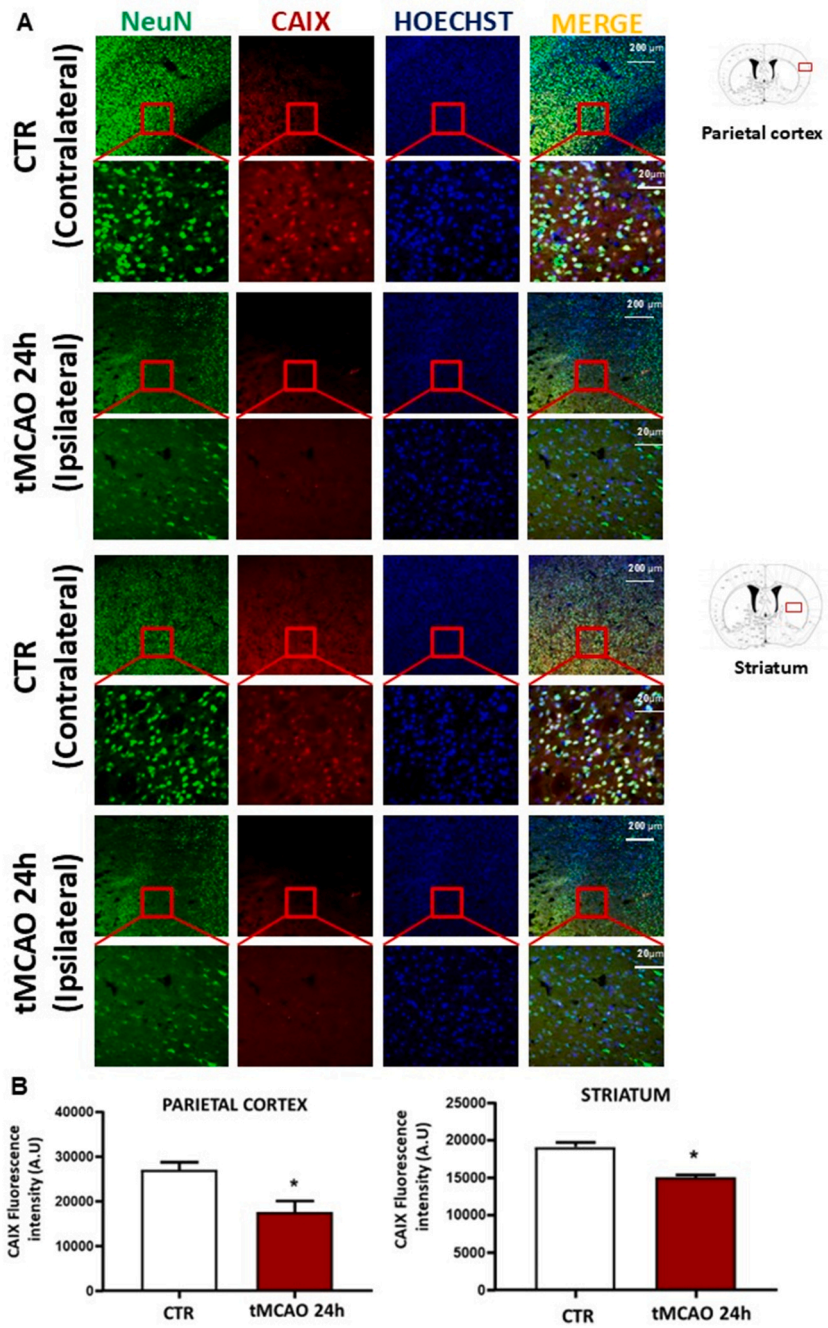

Fig. 6. Immunofluorescence-based characterization of CA IX expression in selected brain regions from rats exposed to the tMCAO setting for 24 h. (A) Immunofluorescence analysis of CA IX in control non-ischemic rats (contralateral) and 24h after stroke induction with 24 h tMCAO (ipsilateral). NeuN (green), CA IX (red), Hoechst (blue), and merged images are represented for each experimental condition. Cartoons on the right side indicate the brain regions examined (cortex, top panels; striatum, lower panels). (B) Quantification of CAIX fluorescence intensity in arbitrary units (AU). Data are expressed as mean ± SEM (n = 3 per group). *p < 0.05 Error bars represent ± SEM; statistical significance was assessed using a *t*-test, df = 4.

1.4. CA IX inhibition is neuroprotective in a rat model of ischemia

In order to verify the potential of C18 as a pharmacologic agent in ischemia in living animals, we administered C18 at a dose of 5 mg/kg via intracerebroventricular (ICV) injection twice (100 min and 3 h after tMCAO in rats). The results showed that ischemic volumes were reduced by half in the C18-treated animals, compared to those treated with vehicle alone (Fig. 8A). Additionally, the

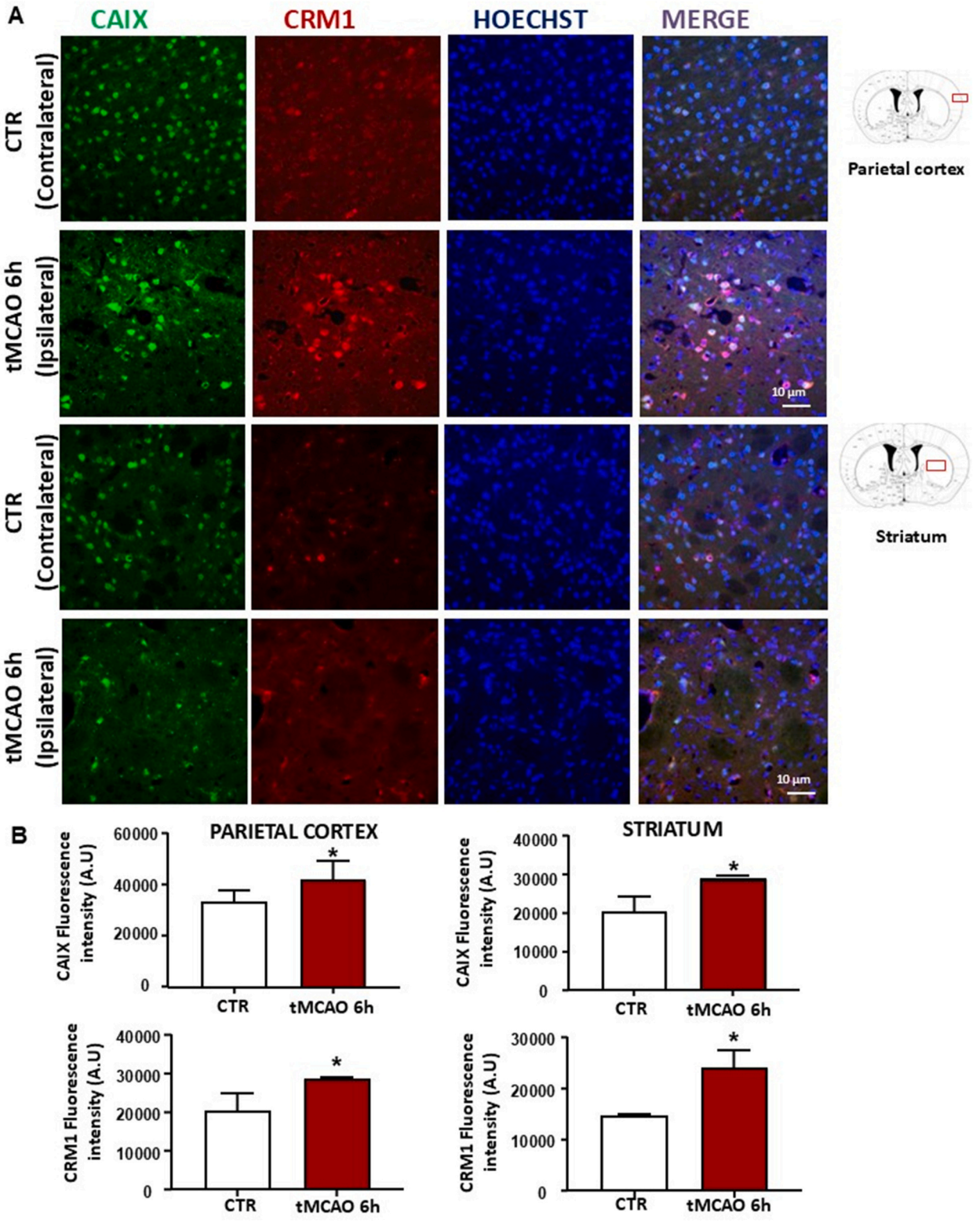

(caption on next page)

Fig. 7. Immunofluorescence-based characterization of the expression of CA IX and its interactor, CRM1, in selected brain regions from rats exposed to early tMCAO (6 h). (A) Immunofluorescence analysis of CA IX in control non-ischemic rats (contralateral) and 6 h after stroke induction with tMCAO (ipsilateral). CRM1 (red), CA IX (green), Hoechst (blue), and merged images are represented for each experimental condition. Cartoons on the right side indicate the brain regions examined (cortex, top panels; striatum, lower panels). (B) Quantification of CA IX and CRM1 fluorescence intensity, arbitrary units (AU). Data are expressed as mean ± SEM (n = 3 for each group). *p < 0.05 Error bars represent ± SEM; statistical significance was assesses using a *t*-test, df = 4.

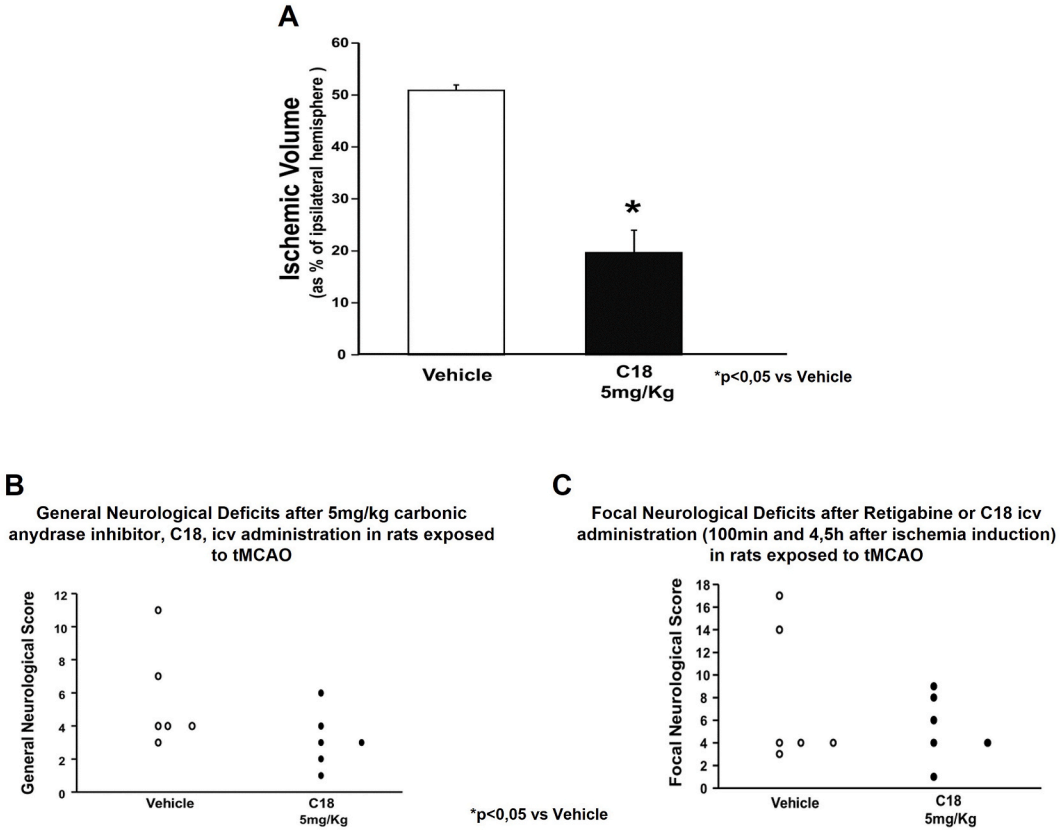

Fig. 8. (A) Ischemic volume and neurological score of rats treated with 5 mg/kg of C18 and subjected to tMCAO for 60'. Ischemic volume is represented as percentage of the ipsilateral hemisphere. (B) Neurological score of rats treated with C18 alone and underwent tMCAO. (C) Neurological score of rats treated with C18 and after retigabine administration.

C18-treated rats exhibited lower general and focal neurological scores (Fig. 8B and C), strengthening the detrimental role of CA IX during brain ischemia and highlighting the potential of CAIs to reduce post-ischemic neurological deficits.

To link these findings to changes in protein levels associated with post-ischemic events, we performed immunoblot analysis on representative samples from striatum and cortex of C18-treated rats subjected to tMCAO (Fig. 9). We observed a generalized decrease in protein expression in the in the ipsilateral brain areas 24 h post-tMCAO, compared to the contralateral ones; consistent with the extent of brain damage consequent to the ischemia. Thus, CA family members CA IX and CA II actually showed decreased protein expression, in agreement with the immunofluorescence data. Intriguingly, CA XII showed a putative compensatory increase in protein levels. Additionally, NFkB, Cleaved-Casp3, SOD1, and nNOS proteins similarly were downregulated in both the ipsilateral cortex and striatum compared to the corresponding contralateral samples. The chaperone BiP levels remained constant across all the samples, indicating that endoplasmic reticular stress was not a factor in the observed changes in protein expression.

2. Discussion

Although stroke is a complex disorder with many contributing factors, several common features can be modeled in experimental stroke studies. One key component is the evolving brain damage, explained by the "penumbra" concept, which depends on factors such as the duration and severity of the insult, collateral systems, as well as age, sex, and comorbidities. It is immediately obvious that experimental models of stroke can only capture specific aspects of this multifaceted disease. Nevertheless, ischemic volume and certain neurological outcomes can be effectively measured in animal models. Despite their productiveness, animal models do have limitations

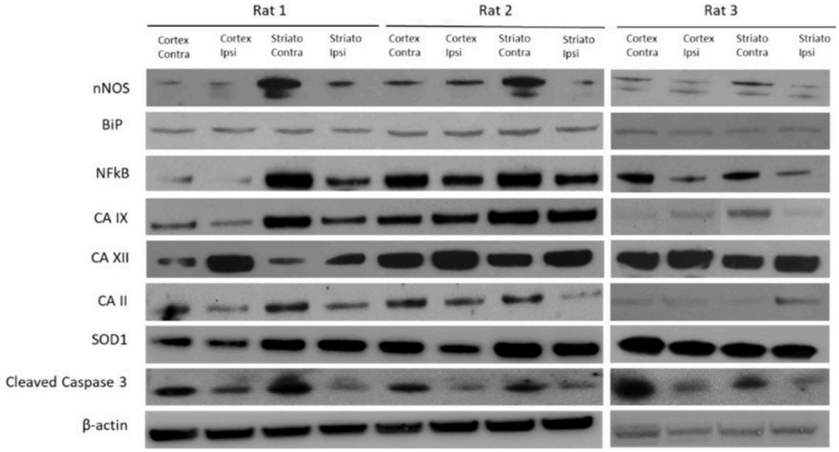

Fig. 9. Protein analysis of CAs, inflammation, apoptosis, oxidative stress markers. For each rat treated with C18 contralateral (contra) and ipsilateral (ipsi) samples for both cortex and striatum are shown. Analysed proteins are listed based on their molecular weight: nNOS, BiP, NFkB, CA IX, CA XII, CA II, SOD1, Cleaved Caspase3, and β-actin (used as control). The uncropped images are provided in the supplementary materials.

in fully replicating human brain ischemia. One major limitation is the potential failure to translate experimental findings into clinical success, which may arise from insufficient understanding of whether the therapeutic targets are present and regulated in human stroke. In this context, analyzing human brain tissues from stroke patients could provide valuable insights, but such studies are challenging due to the limited availability of appropriate brain banks [29]. On the other hand, *in vitro* studies provide fundamental insights into the molecular pathways induced by ischemia-like conditions. While the complexity of ischemic stroke cannot be fully replicated in an *in vitro* system, these models are valuable for investigating specific biochemical and molecular mechanisms associated with energy deficiency similar to ischemia [30]. It is noteworthy that the use of both *in vitro* and *in vivo* models can enhance the identification of potential therapeutic targets with greater confidence. In our hands, the convergence of results from both *in vivo* and *in vitro* models supports the identification of CA IX as a promising druggable target for stroke. Despite the limitations of these models, the evidence gathered suggests that exploring CA IX as a target could pave the way for developing new pharmacological strategies. Human CA IX is canonically described as a hypoxia-induced transmembrane protein within the α-CA enzyme family. It has a crucial role in pH regulation, especially in hypoxic cells, and acts in concert with intracellular CAs to buffer intracellular acidosis induced by hypoxia, which results in extracellular pH acidification. This strategy is usually employed by tumour cells to evade immune surveillance, to enhance invasiveness and resistance to chemo- and radiotherapy. In normal tissues, CA IX expression is tightly controlled by oxygen levels: it is almost undetectable under normoxia but heavily induced by hypoxia. In fact, CA IX is a major effector of HIF-1α activity in the metabolic adaptation of hypoxic tumours, the so-called Warburg effect, and its expression in tumor samples is generally linked to a worse prognosis. HIF-1α is a key transcription factor involved in the ischemic brain. Under normal oxygen levels, HIF-1α undergoes polyubiquitination and degradation [42]. In various brain pathologies, HIF-1α can have either harmful or beneficial effects, depending on the context. For instance, during stroke, HIF-1α is stabilized and drives the transcription of several target genes, including IL-1β, TNFα, and TGF-β. On the other hand, accumulating evidence indicate that HIF-1α plays also a crucial role for neuroprotection against ischemic brain injury by inducing ischemic tolerance [43–45]. Collectively, pharmacological modulation of HIF-1α and its downstream pathways should be considered for future therapeutic interventions.

Besides its well-known membrane role in cancer, CA IX may also be involved in additional physio-pathological processes connected to pH and CO_2 homoeostasis [46,47]. Among these, it is worth mentioning cerebral ischemia. During ischemic events, cerebral acidosis contributes to neuronal injury by generating free radicals, affecting glutamate uptake, and inducing neuronal apoptosis. Despite the advances in the comprehension of the pathophysiology of cerebrovascular injury, the outright stroke treatment remains an important unmet medical need, and research is struggling to identify adequate therapeutic and preventive measures.

Due to the role of CAs in pH and body volume regulation, targeting these enzymes with inhibitors might offer a potential strategy to manage ischemia, in synergy with CAIs function as diuretics. Indeed, previous studies have explored the potential protective effects of CA inhibition in brain ischemia, showing that CAIs can help restore the structure of the ischemic cortex and striatum, mitigate neuronal and astrocyte loss, and reduce microglia activation [26,27].

Starting from these findings, we aimed to further characterize the potential involvement of CA IX in ischemic damage, using both *in vitro* and in *vivo* approaches. In particular, we exploited loss-of-function strategies, including genetic knock-out models and *bona fide* enzyme inhibition with the membrane-impermeant C18, to verify complementary results.

We firstly showed that CA IX subcellular distribution in rat-derived primary neurons exposed to OGD/Rx varies: its levels increased on plasma membrane after OGD, with the exacerbation of nuclear localization after OGD/Rx [48]. This suggests that CA IX trafficking is associated with cellular responses to these stress conditions. Interestingly, the observed nuclear accumulation of CA IX after OGD/Rx, possibly due to interactions with nucleo-cytoplasmic transport ligands [49,50], recalls involvement in nucleolar stress events, which are associated with a general decrease in protein synthesis following hypoxic exposure [51].

The weak phenotypes which characterize *Car9* knock-out mice imply that more pronounced effects might emerge under stress

conditions such as brain ischemia. The *Car9* −/− mice allowed us to perform *in vitro* studies on both neuronal and non-neuronal cell cultures. Interestingly, mice-derived primary neuronal cultures revealed not only the harmful role of CA IX in cell survival but also that this phenomenon can be selectively relevant in neurons and not in other cell types (i.e., stabilized mouse embryo fibroblasts, data not shown). This indicates the potential tissue-specificity of the observed phenomena.

Considering the ongoing efforts to discovering and characterize CAIs, particularly for tumours overexpressing the prognosis marker CA IX, and given that genetic inhibition may only provide proof-of-concept evidence for targeting CA IX in ischemic stroke, we shifted our focus toward the evaluation of CA IX enzyme inhibition directly. We concentrated on the availability of the cell-impermeant CAI, C18 [1]. In virtue of its positive charge, it is not able to cross the cellular membranes and, therefore, was described for the first time as a putative selective inhibitor of membrane associated CAs, including CA IX. Remarkably, the behaviour of *Car9* KO cortical neurons was phenocopied by C18 inhibition in OGD/Rx cortical neurons, with the efficacy being dose dependent. The inhibition was effective only in wild-type neurons, thus indicating that CA IX is a main contributor to the observed increased neuronal survival.

We then conducted *in vivo* experiments in rats exposed to tMCAO. As a starting point, we focused on the striatum and motor cortex as the most suitable regions for the analysis, due to their high levels of CA IX expression and potential susceptibility to its effects. In fact, CA IX is barely expressed within the brain as, according to publicly available RNAseq analysis (https://www.proteinatlas.org/), only a limited fraction of cells in the normal brain express CA IX [52]. In both regions, CA IX expression decreased at 24h post tMCAO. Additionally, co-localization with exportin-1 was evident 6 h after the treatment, as a possible marker of an active stressful condition associated to hypoxia, as seen in cultured cells [51]. Taken together, these results suggest that inhibition CA IX plays relevant roles in OGD/Rx stress and could offer neuroprotection following ischemic brain re-oxygenation. Moreover, CA IX nuclear function might mediate its detrimental effect during ischemic insult.

Furthermore, C18-mediated CA inhibition resulted neuroprotective *in vivo* in rat models of ischemia, evidenced by reduction of ischemic volume and neurological deficits. It is expected that damage to the blood-brain barrier consequent to ischemic insults may facilitate the access of C18 to the damaged areas.

Protein analysis in this context showed interesting, though unexpected, results. Indeed, we noted intriguing decreases in key proteins associated with ischemic pathways, including inflammation (NFkB), apoptosis (Cl-Cas3), oxidative stress (SOD1), and neurotoxicity (nNOS). In countertendency, CA XII was the only protein to show overexpression, likely indicating a compensatory mechanism. The contribution of different subcellular populations in the brain, their interaction with other carbonic anhydrases (CAs), and whether these effects are CA IX-dependent remain to be elucidated.

Our study supports previously reported neuroprotective effects of CA inhibition [53], with a particular focus on CA IX, and offers insights into CA IX's dynamic localization changes during ischemic conditions. This adds a novel dimension to our understanding of CA IX role in ischemia, highlighting how its shifting localization might influence its impact on neuronal survival. The variability in CA IX expression across various brain regions also implies that the effects of CA IX inhibition on ischemic conditions will differ depending on the regional expression patterns. Understanding these regional dynamics is crucial for developing targeted and effective therapies for brain ischemia. Effective treatment strategies should account for these differences to maximize therapeutic benefits and minimize potential risks. However, the current evidence is still preliminary, and further investigation is needed to fully understand the molecular mechanisms underlying the neuroprotective effects of CA IX inhibition.

2.1. Conclusion

Current treatments for ischemic stroke focus on acute treatment, secondary prevention, and rehabilitation. CA IX inhibition offers a new approach by targeting the metabolic and pH imbalances resulting from ischemia, potentially enhancing existing therapies and improving patient outcomes. Our use of loss-of-function strategies, combining enzyme inhibition and genetic knock-out has deepened the knowledge on CA IX's contribution to hypoxic insults *in vitro*. We dissected a relevant role for CA IX in ischemia through an established murine model of genetic ablation. In rodent neuronal primary cultures under OGD/Rx, we highlighted CA IX negative impact on neuronal survival. In rat models of brain ischemia, we verified the suitability of C18 to improve recovery after tMCAO, with significant effects on reducing ischemic volumes and improving neurological deficits. Although our findings in rodent models suggest CA IX inhibition as a potential therapeutic strategy, further studies are required to validate the preclinical evidence for the suitability of future applications to stroke in humans.

3. Materials and methods

3.1. Animals

For the present study, *Mus musculus Car9 Knock-out* in the C57BL/6JOlaHsd genetic background and male Sprague Dawley rats were used. The animals with inactivating mutation of the *Car9* gene have previously been generated and described [40]. The animals included in this study were housed using procedures described in the Jackson Lab Resource Handbook. *In vitro* and *in vivo* experiments were performed according to the international guidelines for animal research and approved by the Animal Care Committee of "Federico II" University of Naples, Italy and Ministry of Health, Italy (Authorizations #89/2019-PR; #731/2022, #907/2023-PR). For any surgical or invasive procedure, in compliance with the inherent regulations, animals were anesthetized using sevoflurane at 3.5 % (Medical Oxygen Concentrator LFY-I-5A) mixed with oxygen. Euthanasia was performed with an overdose of sevoflurane at 6h or at 24h post-tMCAO to evaluate infarct volume or protein expression.

3.2. Primary cortical neurons

Rat primary cortical neurons were taken from E17.5 Wistar rat embryos (Charles River). Dissection and dissociation were performed in Ca^{2+}/Mg^{2+}-free PBS with 30 mM glucose. Tissues were incubated with papain at 37 °C for 10 min and dissociated by trituration in Earle's balanced salt solution (EBSS) containing 0.16 U/mL DNase, 10 mg/mL BSA 10 mg/mL, and 10 mg/mL ovomucoid. Neurons were thus plated on Petri dishes coated with poly-d-lysine 20 μg/mL, and were grown in DMEM/F12 with glucose, 5 % FBS and 5 % horse serum, 2 mM glutamine, 50 U/mL penicillin and 50 μg/mL streptomycin. To prevent non-neuronal cell growth 10 μM arabinoside-C was added within 48h. Neurons were cultured at 37 °C in a humidified 5 % CO_2 atmosphere and used after 7–10 days of culture [54]. Using the same procedure, mouse primary cortical neurons were collected from E17.5 C57BL/6JOlaHsd mice WT and strain-matched *Car9*- KO.

3.3. Treatments

Oxygen and glucose deprivation (OGD) was performed for 3h in a hypoxic chamber with a medium containing NaCl 116 mM, KCl 5.4 mM, $MgSO_4$ 0.8 mM, $NaHCO_3$ 26.2 mM, NaH_2PO_4 1 mM, $CaCl_2$ 1.8 mM, glycine 0.01 mM. At the end of incubation, cells were removed from the hypoxic chamber, and the glucose-free medium was replaced with a medium containing normal levels of O_2 and glucose. Reoxygenation (Rx) was achieved by returning neurons to normoxic conditions (5 % CO_2 and 95 % air) for 24 h [54].

For enzyme inhibition, C18 was dissolved in DMSO 20 % in PBS and used at the following concentrations: 3 nM, 10 nM, and 30 nM. Acetazolamide was dissolved in DMSO 20 % in PBS and used at a final concentration of 1 mM. DMSO 20 % in PBS was used as negative control.

3.4. Cell viability assay

Neuronal viability was assessed as mitochondrial activity by the MTT (3[4,5-dimethylthiazol-2-yl]-2,5-diphenyl-tetrazolium bromide) assay. Briefly, after treatments, neurons were incubated with a 0.5 mg/mL MTT solution at 37 °C for 1 h, then collected in DMSO. Once dissolved, absorbance was determined spectrophotometrically at 540 nm. Data were expressed as a percentage of cell viability relative to controls.

3.5. Tissue processing, immunostaining, and confocal immunofluorescence

Brain tissues were collected from euthanized rats as reported below. Contralateral and ipsilateral striatum and cortex were removed, weighted, and cryopreserved al −20 °C for protein analysis. Proteins were lysed as previously reported [55], with the substitution of NP-40 detergent with Triton X-100, in the presence of a cocktail of protease inhibitors (Sigma Aldrich). Briefly, 6 vol (w/v) of ice-cold lysis buffer were added in a glass Dounce, and manual homogenization was carried out until the compound was homogeneous. Lysates were clarified by centrifugation at 12,000 g for 20 min at 4 °C, the supernatant was collected and quantified with BioRad Protein Assay, based on the Bradford method, using a standard curve of BSA and according to manufacturer's instructions. Protein samples (30 μg each) were resolved by SDS-PAGE, on NuPAGE Bis-Tris 4–12 % gradient gels (Invitrogen), transferred onto a PVDF membrane (Millipore), and blocked with 5 % non-fat milk.

Target proteins were detected using the following primary antibodies: monoclonal mouse anti-CA IX M75 (1:300); mouse monoclonal anti-GRP78 (1:100) (Santa Cruz Biotechnology); polyclonal rabbit anti-BiP #3183 (1:1000) (Cell Signalling technologies); polyclonal rabbit anti-Cleaved Caspase-3 (Asp175) #9661 (Cell Signalling technologies); monoclonal rabbit anti-nNOS #4231 (C7D7) (1:1000) (Cell Signalling technologies); monoclonal rabbit anti-SOD1 (E4G1H) #37385 (1:1000) (Cell Signalling technologies); mouse monoclonal anti-CA II (G-2) sc-48351 (1:1000) (Santa Cruz Biotechnology); rabbit monoclonal NF-κB p65 (D14E12) #8242 (1:1000) (Cell Signalling technologies); mouse monoclonal anti-CA XII (A-3) sc-374313 (1:1000) (Santa Cruz Biotechnology); rabbit polyclonal anti- CA IX (PA5-77885) (1:1000) (Invitrogen), mouse monoclonal anti-beta actin sc-81178 (1:2000) (Santa Cruz Biotechnology). Then, the respective peroxidase-conjugated anti-mouse secondary antibody (1:10,000) (Santa Cruz Biotechnology) or anti-rabbit secondary antibody (1:5000) (Santa Cruz Biotechnology) was used. Immunoreactive bands were detected by ECL (Amersham) and acquired with a Chemi Doc Imaging System (BioRad) or with X-ray films (Fujifilm).

Rat primary cortical neurons were fixed at room temperature in 4 % (w/v) paraformaldehyde for 20 min and washed 3 times with PBS. Brain sections were incubated in proteinase K buffer containing 1 M Tris-HCl (pH 7.4), 0.5 M EDTA, 5 M NaCl, and proteinase K (15 μg/mL) in RNase-free water at 37 °C for 10 min, rinsed three times for 3 min in PBS. To reduce nonspecific signal, rat primary cortical neurons were treated with 1 % BSA in PBS for 30 min, whereas brain sections were blocked with a solution containing 2 % sheep serum and 1 % BSA in PBS with 0.1 % Tween-20 for 15 min at room temperature. Cells were then incubated for 2h with specific primary antibodies in humidified chamber. Rat primary cortical neurons were incubated with anti-CA9 H-120 (1:100) (Santa Cruz Biotechnology) rabbit polyclonal and βIII tubulin (1:200) (Santa Cruz Biotechnology). After washing three times for 3 min in PBS, brain sections were incubated with the following primary antibodies in blocking solution: anti-NeuN (1:200) (Elabscience), anti-CA9 H-120 (1:100) (Santa Cruz Biotechnology) rabbit polyclonal and mouse monoclonal anti-CRM1 (C-1) sc-74454 (Santa Cruz Biotechnology) overnight. To visualize the targeted proteins by fluorescence, after 3 washes with PBS, samples were incubated in humidified chamber for 1h (cells) and 2h (tissues) with secondary antibodies Alexa-488-conjugated donkey anti-mouse, Alexa-488-conjugated donkey anti-rabbit (1:200) (Jackson Laboratories), Alexa-546-conjugated donkey anti-mouse and Alexa-546-conjugated donkey anti-rabbit (1:200) (Jackson Laboratories). Finally, cell nuclei were marked with Hoechst staining (1:3000) for 20 min and

washed two times with PBS. Cells were mounted onto microscope slides with Glycerol/PBS 1:1; sections were mounted onto slides using Fluoromount aqueous mounting medium (Sigma). Both were air-dried and stored in a dark room. Fluorescence was observed using a Zeiss LSM 700 laser scanning confocal microscope. Each experiment was performed in triplicate and 30 fields for each experimental condition were analysed for representativeness of the reported findings. Analyses were performed using Image J software in the total number of positive signals of CAIX antibodies for photographic field (mm^2) for each condition.

Animals were anesthetized and transcardially perfused with a saline solution containing 0.01 mL heparin, followed by 4 % paraformaldehyde in PBS. Brains were processed as previously described [56]. Brains were rapidly removed on ice and postfixed overnight at 4 °C and cryoprotected in 30 % sucrose in 0.1 M phosphate buffer (PB) with sodium azide 0.02 % for 24 h at 4 °C. Next, brains were sectioned frozen on a sliding cryostat at 20 μm thickness, in rostrum-caudal direction. Afterward, free-floating serial sections were incubated with PB Triton X 0.3 % and blocking solution (0.5 % milk, 10 % FBS, 1 % BSA) for 1 h and 30 min. The sections were incubated overnight at +4 °C with the following primary antibodies: anti-CA9 H-120 (1:100) (Santa Cruz Biotechnology), anti-CRM1 (C-1) sc-74454, anti-NeuN (Millipore). The sections were then incubated with the corresponding fluorescent-labeled secondary antibodies, Alexa 488/Alexa 594 conjugated anti-mouse/anti-rabbit IgG. Nuclei were counterstained with Hoechst. Images were observed using a Zeiss LSM700 META/laser scanning confocal microscope (Zeiss, Oberkochen, Germany). Single images were taken with a resolution of 1024 × 1024. Cortex and striatum images from the same areas of each brain region were compared. Analyses were performed using Image J software in the total number of positive signals of CAIX and CRM1 antibodies for photographic field (mm^2) in parietal cortex and striatum of control and tMCAO. n = 3 mice per treatment group [57].

3.6. Transient middle cerebral artery occlusion (tMCAO) and drug administration

Transient focal ischemia was induced in anesthetized rats by middle cerebral artery occlusion for 100 min [58,59]. In brief, under an operating stereomicroscope Nikon SMZ800 (Nikon Instruments), a 5-0 surgical monofilament nylon suture was introduced through the right external carotid artery into the circle of Willis for 19 mm to reach the origin of middle cerebral artery (MCA), thus blocking blood flow through the artery. To confirm the achievement of ischemia, cerebral blood flow was monitored through a disposable microtip fiber optic probe (diameter 0.5 mm) connected through a master probe to a laser Doppler computerized main unit (PF5001) and analysed using PSW Perisoft 2.5. C18 (5 mg/kg) was administered intracerebroventricularly twice: 100 min and 3h after ischemia induction in rats exposed to tMCAO.

3.7. Neurological scores

Neurological scores were evaluated according to the general and focal neurological scales. For the general neurological score, the conditions of the hair, position of ears, conditions of the eyes, posture, spontaneous activity on the bench, and the presence of epileptic behaviour were measured. The obtained scores were then summed to have a general neurological score, ranging between 0 and 28 depending on the severity of signs. For the focal neurological score, the symmetry of the body, gait, the ability to climb, the presence of circling behaviour, front limb asymmetry, compulsory circling, and whisker response were considered. The focal neurological score was then obtained by the addition of each component [59].

3.8. Evaluation of the infarct volume

The evaluation of the infarct volume was performed as previously described [59]. Briefly, before euthanasia animals were perfused transcardially under deep anesthesia with 0,9 % saline solution, followed by 4 % paraformaldehyde (Sigma) in phosphate-buffered saline. The brains were removed and postfixed overnight at 4 °C and cryoprotected in 30 % sucrose phosphate buffer saline. Frozen brains were sectioned with a sliding cryostat at 40 μm thickness and Nissl staining was performed. Infarct volume was calculated by summing the infarction areas of all sections and by multiplying the total by slice thickness. To avoid the bias caused by the presence of oedema, the infarct volume was expressed as a percentage of the infarct volume of the total ipsilateral hemispheric volume.

3.9. Statistical analyses

Statistical comparisons between groups were performed by unpaired *t*-test or by one-way ANOVA followed by Newman-Keuls' test or Tukey's multiple comparisons test. Neurological scores were analysed using the non-parametric Kruskal-Wallis test, followed by Dunn's multiple comparison test.

CRediT authorship contribution statement

Sara Amiranda: Writing – original draft, Investigation, Data curation. **Mariangela Succoio:** Writing – original draft, Investigation, Conceptualization. **Serenella Anzilotti:** Methodology, Investigation, Conceptualization. **Ornella Cuomo:** Methodology, Investigation. **Tiziana Petrozziello:** Methodology, Investigation. **Valentina Tedeschi:** Methodology, Investigation. **Arianna Finizio:** Methodology, Investigation. **Giorgia Mele:** Methodology. **Seppo Parkkila:** Writing – review & editing, Conceptualization. **Lucio Annunziato:** Conceptualization. **Giuseppina De Simone:** Writing – review & editing, Conceptualization. **Giuseppe Pignataro:** Writing – review & editing, Investigation, Conceptualization. **Agnese Secondo:** Writing – review & editing, Writing – original draft,

Investigation, Funding acquisition, Conceptualization. **Nicola Zambrano:** Writing – review & editing, Writing – original draft, Project administration, Investigation, Funding acquisition, Data curation, Conceptualization.

Ethics statement

In vivo experiments were approved by the Animal Care Committee of "Federico II" University of Naples, Italy and Ministry of Health, Italy (Authorizations #89/2019-PR; #731/2022, #907/2023-PR); they were performed according to the international guidelines for animal research and in compliance with the inherent regulations.

Funding

This work was supported by the Ministero dell'Università e della Ricerca, Italy, under Grant PRIN number 2015KRYSJN to AS and NZ.

Declaration of competing interest

The authors declare the following financial interests/personal relationships which may be considered as potential competing interests: Nicola Zambrano, PhD, currently serves in a Section Editor activity for Heliyon Biochemistry, Molecular and Cell Biology If there are other authors, they declare that they have no known competing financial interests or personal relationships that could have appeared to influence the work reported in this paper.

Acknowledgments

The Authors are indebted to Prof. Claudiu T. Supuran for critical discussion and for providing the positively charged pyridinium sulfonamide C18 and acetazolamide. The Authors also thank Prof. Giovanna Maria Pierantoni for contribution to immunofluorescence experiments of brain samples and their quantitation.

Appendix A. Supplementary data

Supplementary data to this article can be found online at https://doi.org/10.1016/j.heliyon.2025.e42457.

References

[1] C.T. Supuran, Carbonic anhydrases: novel therapeutic applications for inhibitors and activators, Nat. Rev. Drug Discov. 7 (2008) 168–181, https://doi.org/10.1038/nrd2467.
[2] V. Alterio, et al., Crystal structure of the catalytic domain of the tumor-associated human carbonic anhydrase IX, Proc. Natl. Acad. Sci. U. S. A. 106 (2009) 16233–16238, https://doi.org/10.1073/pnas.0908301106.
[3] S. Pastorekova, R.J. Gillies, The role of carbonic anhydrase IX in cancer development: links to hypoxia, acidosis, and beyond, Cancer Metastasis Rev. 38 (2019) 65–77, https://doi.org/10.1007/s10555-019-09799-0.
[4] C.T. Supuran, How many carbonic anhydrase inhibition mechanisms exist? J. Enzym. Inhib. Med. Chem. 31 (2016) 345–360, https://doi.org/10.3109/14756366.2015.1122001.
[5] M. Kciuk, et al., Targeting carbonic anhydrase IX and XII isoforms with small molecule inhibitors and monoclonal antibodies, J. Enzym. Inhib. Med. Chem. 37 (2022) 1278–1298, https://doi.org/10.1080/14756366.2022.2052868.
[6] C.T. Supuran, A. Di Fiore, V. Alterio, S.M. Monti, G. De Simone, Recent advances in structural studies of the carbonic anhydrase family: the crystal structure of human CA IX and CA XIII, Curr. Pharm. Des. 16 (2010) 3246–3254, https://doi.org/10.2174/138161210793429841.
[7] V. Alterio, A. Di Fiore, K. D'Ambrosio, C.T. Supuran, G. De Simone, Multiple binding modes of inhibitors to carbonic anhydrases: how to design specific drugs targeting 15 different isoforms? Chem. Rev. 112 (2012) 4421–4468, https://doi.org/10.1021/cr200176r.
[8] V. Alterio, D. Esposito, S.M. Monti, C.T. Supuran, G. De Simone, Crystal structure of the human carbonic anhydrase II adduct with 1-(4-sulfamoylphenyl-ethyl)-2,4,6-triphenylpyridinium perchlorate, a membrane-impermeant, isoform selective inhibitor, J. Enzym. Inhib. Med. Chem. 33 (2018) 151–157, https://doi.org/10.1080/14756366.2017.1405263.
[9] V. Alterio, et al., Carbonic anhydrase inhibitors: X-ray and molecular modeling study for the interaction of a fluorescent antitumor sulfonamide with isozyme II and IX, J. Am. Chem. Soc. 128 (2006) 8329–8335, https://doi.org/10.1021/ja061574s.
[10] V. Menchise, et al., Carbonic anhydrase inhibitors: stacking with Phe131 determines active site binding region of inhibitors as exemplified by the X-ray crystal structure of a membrane-impermeant antitumor sulfonamide complexed with isozyme II, J. Med. Chem. 48 (2005) 5721–5727, https://doi.org/10.1021/jm050333c.
[11] G. De Simone, V. Alterio, C.T. Supuran, Exploiting the hydrophobic and hydrophilic binding sites for designing carbonic anhydrase inhibitors, Expet Opin. Drug Discov. 8 (2013) 793–810, https://doi.org/10.1517/17460441.2013.795145.
[12] G. Ilardi, et al., Histopathological determinants of tumor resistance: a special look to the immunohistochemical expression of carbonic anhydrase IX in human cancers, Curr. Med. Chem. 21 (2014) 1569–1582, https://doi.org/10.2174/09298673113209990227.
[13] C. Miro, et al., Thyroid hormone enhances angiogenesis and the Warburg effect in squamous cell carcinomas, Cancers 13 (2021), https://doi.org/10.3390/cancers13112743.
[14] A.L. Harris, Hypoxia–a key regulatory factor in tumour growth, Nat. Rev. Cancer 2 (2002) 38–47, https://doi.org/10.1038/nrc704.
[15] G. Pignataro, R.P. Simon, Z.G. Xiong, Prolonged activation of ASIC1a and the time window for neuroprotection in cerebral ischaemia, Brain 130 (2007) 151–158, https://doi.org/10.1093/brain/awl325.
[16] S. Paul, E. Candelario-Jalil, Emerging neuroprotective strategies for the treatment of ischemic stroke: an overview of clinical and preclinical studies, Exp. Neurol. 335 (2021) 113518, https://doi.org/10.1016/j.expneurol.2020.113518.

[17] F. Erra Diaz, E. Dantas, J. Geffner, Unravelling the interplay between extracellular acidosis and immune cells, Mediat. Inflamm. (2018) 1218297, https://doi.org/10.1155/2018/1218297(2018).
[18] F. Plum, What causes infarction in ischemic brain?: the Robert Wartenberg Lecture, Neurology 33 (1983) 222–233, https://doi.org/10.1212/wnl.33.2.222.
[19] C.T. Supuran, Applications of carbonic anhydrases inhibitors in renal and central nervous system diseases, Expert Opin. Ther. Pat. 28 (2018) 713–721, https://doi.org/10.1080/13543776.2018.1519023.
[20] L. Velisek, S.L. Moshe, P.K. Stanton, Resistance of hippocampal synaptic transmission to hypoxia in carbonic anhydrase II-deficient mice, Brain Res. 671 (1995) 245–253, https://doi.org/10.1016/0006-8993(94)01336-g.
[21] C.C. Wykoff, et al., Hypoxia-inducible expression of tumor-associated carbonic anhydrases, Cancer Res. 60 (2000) 7075–7083.
[22] D.P. Stiehl, et al., Increased prolyl 4-hydroxylase domain proteins compensate for decreased oxygen levels. Evidence for an autoregulatory oxygen-sensing system, J. Biol. Chem. 281 (2006) 23482–23491, https://doi.org/10.1074/jbc.M601719200.
[23] S. Kaluz, M. Kaluzova, S.Y. Liao, M. Lerman, E.J. Stanbridge, Transcriptional control of the tumor- and hypoxia-marker carbonic anhydrase 9: a one transcription factor (HIF-1) show? Biochim. Biophys. Acta 1795 (2009) 162–172, https://doi.org/10.1016/j.bbcan.2009.01.001.
[24] E.M. Kniep, et al., Inhibition of apoptosis and reduction of intracellular pH decrease in retinal neural cell cultures by a blocker of carbonic anhydrase, Investig. Ophthalmol. Vis. Sci. 47 (2006) 1185–1192, https://doi.org/10.1167/iovs.05-0555.
[25] M.R. Williamson, C.M. Wilkinson, K. Dietrich, F. Colbourne, Acetazolamide mitigates intracranial pressure spikes without affecting functional outcome after experimental hemorrhagic stroke, Transl Stroke Res 10 (2019) 428–439, https://doi.org/10.1007/s12975-018-0663-6.
[26] L. Di Cesare Mannelli, et al., Carbonic anhydrase inhibition for the management of cerebral ischemia: in vivo evaluation of sulfonamide and coumarin inhibitors, J. Enzym. Inhib. Med. Chem. 31 (2016) 894–899, https://doi.org/10.3109/14756366.2015.1113407.
[27] I. Bulli, et al., Role of carbonic anhydrase in cerebral ischemia and carbonic anhydrase inhibitors as putative protective agents, Int. J. Mol. Sci. 22 (2021), https://doi.org/10.3390/ijms22095029.
[28] I. Dettori, et al., Protective effects of carbonic anhydrase inhibition in brain ischaemia in vitro and in vivo models, J. Enzym. Inhib. Med. Chem. 36 (2021) 964–976, https://doi.org/10.1080/14756366.2021.1907575.
[29] C.J. Sommer, Ischemic stroke: experimental models and reality, Acta Neuropathol. 133 (2017) 245–261, https://doi.org/10.1007/s00401-017-1667-0.
[30] P.M. Holloway, F.N. Gavins, Modeling ischemic stroke in vitro: status quo and future perspectives, Stroke 47 (2016) 561–569, https://doi.org/10.1161/STROKEAHA.115.011932.
[31] W. Liu, et al., Senescence marker protein 30 confers neuroprotection in oxygen-glucose deprivation/reoxygenation-injured neurons through modulation of Keap1/Nrf2 signaling: role of SMP30 in OGD/R-induced neuronal injury, Hum. Exp. Toxicol. 40 (2021) 472–482, https://doi.org/10.1177/0960327120954243.
[32] Y.Y. Wang, et al., Piezo1 mediates neuron oxygen-glucose deprivation/reoxygenation injury via Ca(2+)/calpain signaling, Biochem. Biophys. Res. Commun. 513 (2019) 147–153, https://doi.org/10.1016/j.bbrc.2019.03.163.
[33] E. Gouix, et al., Oxygen glucose deprivation-induced astrocyte dysfunction provokes neuronal death through oxidative stress, Pharmacol. Res. 87 (2014) 8–17, https://doi.org/10.1016/j.phrs.2014.06.002.
[34] F. Boscia, et al., NCX1 expression and functional activity increase in microglia invading the infarct core, Stroke 40 (2009) 3608–3617, https://doi.org/10.1161/STROKEAHA.109.557439.
[35] V. Tedeschi, A. Vinciguerra, M.J. Sisalli, G. Pignataro, A. Secondo, Pharmacological inhibition of lysosomal two-pore channel 2 (TPC2) confers neuroprotection in stroke via autophagy regulation, Neurobiol. Dis. 178 (2023) 106020, https://doi.org/10.1016/j.nbd.2023.106020.
[36] X. Yang, et al., Neuroserpin protects rat neurons and microglia-mediated inflammatory response against oxygen-glucose deprivation- and reoxygenation treatments in an in vitro study, Cell. Physiol. Biochem. 38 (2016) 1472–1482, https://doi.org/10.1159/000443089.
[37] Y. Tian, L. Wang, Z. Qiu, Y. Xu, R. Hua, Autophagy triggers endoplasmic reticulum stress and C/EBP homologous protein-mediated apoptosis in OGD/R-treated neurons in a caspase-12-independent manner, J. Neurophysiol. 126 (2021) 1740–1750, https://doi.org/10.1152/jn.00649.2020.
[38] A. Secondo, et al., Pharmacological characterization of the newly synthesized 5-amino-N-butyl-2-(4-ethoxyphenoxy)-benzamide hydrochloride (BED) as a potent NCX3 inhibitor that worsens anoxic injury in cortical neurons, organotypic hippocampal cultures, and ischemic brain, ACS Chem. Neurosci. 6 (2015) 1361–1370, https://doi.org/10.1021/acschemneuro.5b00043.
[39] N. Chaparro-Cabanillas, et al., Transient middle cerebral artery occlusion model of stroke, J. Vis. Exp. (2023), https://doi.org/10.3791/65857.
[40] M.O. Gut, et al., Gastric hyperplasia in mice with targeted disruption of the carbonic anhydrase gene Car9, Gastroenterology 123 (2002) 1889–1903, https://doi.org/10.1053/gast.2002.37052.
[41] X. Du, et al., Hypoxia-inducible factor 1alpha and 2alpha have beneficial effects in remote ischemic preconditioning against stroke by modulating inflammatory responses in aged rats, Front. Aging Neurosci. 12 (2020) 54, https://doi.org/10.3389/fnagi.2020.00054.
[42] M. Ema, et al., A novel bHLH-PAS factor with close sequence similarity to hypoxia-inducible factor 1alpha regulates the VEGF expression and is potentially involved in lung and vascular development, Proc. Natl. Acad. Sci. U. S. A. 94 (1997) 4273–4278, https://doi.org/10.1073/pnas.94.9.4273.
[43] G.S. Ralph, et al., Identification of potential stroke targets by lentiviral vector mediated overexpression of HIF-1 alpha and HIF-2 alpha in a primary neuronal model of hypoxia, J. Cerebr. Blood Flow Metabol. 24 (2004) 245–258, https://doi.org/10.1097/01.WCB.0000110532.48786.46.
[44] G.L. Semenza, Hypoxia-inducible factors in physiology and medicine, Cell 148 (2012) 399–408, https://doi.org/10.1016/j.cell.2012.01.021.
[45] F.R. Sharp, M. Bernaudin, HIF1 and oxygen sensing in the brain, Nat. Rev. Neurosci. 5 (2004) 437–448, https://doi.org/10.1038/nrn1408.
[46] M. Benej, et al., CA IX stabilizes intracellular pH to maintain metabolic reprogramming and proliferation in hypoxia, Front. Oncol. 10 (2020) 1462, https://doi.org/10.3389/fonc.2020.01462.
[47] G. Rusciano, E. Sasso, A. Capaccio, N. Zambrano, A. Sasso, Revealing membrane alteration in cellsoverexpressing CA IX and EGFR by Surface-Enhanced Raman Scattering, Sci. Rep. 9 (2019) 1832, https://doi.org/10.1038/s41598-018-37997-3.
[48] M. Succoio, et al., Carbonic anhydrase IX subcellular localization in normoxic and hypoxic SH-SY5Y neuroblastoma cells is assisted by its C-terminal protein interaction domain, Heliyon 9 (2023) e18885, https://doi.org/10.1016/j.heliyon.2023.e18885.
[49] P. Buanne, et al., Characterization of carbonic anhydrase IX interactome reveals proteins assisting its nuclear localization in hypoxic cells, J. Proteome Res. 12 (2013) 282–292, https://doi.org/10.1021/pr300565w.
[50] M. Buonanno, et al., Disclosing the interaction of carbonic anhydrase IX with cullin-associated NEDD8-dissociated protein 1 by molecular modeling and integrated binding measurements, ACS Chem. Biol. 12 (2017) 1460–1465, https://doi.org/10.1021/acschembio.7b00055.
[51] E. Sasso, et al., Binding of carbonic anhydrase IX to 45S rDNA genes is prevented by exportin-1 in hypoxic cells, BioMed Res. Int. (2015) 674920, https://doi.org/10.1155/2015/674920(2015).
[52] E. Sjostedt, et al., An atlas of the protein-coding genes in the human, pig, and mouse brain, Science 367 (2020), https://doi.org/10.1126/science.aay5947.
[53] N. Lemon, E. Canepa, M.A. Ilies, S. Fossati, Carbonic anhydrases as potential targets against neurovascular unit dysfunction in alzheimer's disease and stroke, Front. Aging Neurosci. 13 (2021) 772278, https://doi.org/10.3389/fnagi.2021.772278.
[54] M.J. Sisalli, et al., Endoplasmic reticulum refilling and mitochondrial calcium extrusion promoted in neurons by NCX1 and NCX3 in ischemic preconditioning are determinant for neuroprotection, Cell Death Differ. 21 (2014) 1142–1149, https://doi.org/10.1038/cdd.2014.32.
[55] C. Barbato, et al., Interaction of Tau with Fe65 links tau to APP, Neurobiol. Dis. 18 (2005) 399–408, https://doi.org/10.1016/j.nbd.2004.10.011.
[56] S. Anzilotti, et al., Chronic exposure to l-BMAA cyanotoxin induces cytoplasmic TDP-43 accumulation and glial activation, reproducing an amyotrophic lateral sclerosis-like phenotype in mice, Biomed. Pharmacother. 167 (2023) 115503, https://doi.org/10.1016/j.biopha.2023.115503.

[57] L. Sanguigno, et al., Triticum vulgare extract exerts an anti-inflammatory action in two in vitro models of inflammation in microglial cells, PLoS One 13 (2018) e0197493, https://doi.org/10.1371/journal.pone.0197493.
[58] G. Pignataro, et al., The NCX3 isoform of the Na+/Ca2+ exchanger contributes to neuroprotection elicited by ischemic postconditioning, J. Cerebr. Blood Flow Metabol. 31 (2011) 362–370, https://doi.org/10.1038/jcbfm.2010.100.
[59] G. Pignataro, F.E. Studer, A. Wilz, R.P. Simon, D. Boison, Neuroprotection in ischemic mouse brain induced by stem cell-derived brain implants, J. Cerebr. Blood Flow Metabol. 27 (2007) 919–927, https://doi.org/10.1038/sj.jcbfm.9600422.